Frontiers of Information Technology & Electronic Engineering
www.jzus.zju.edu.cn; engineering.cae.cn; www.springerlink.com
ISSN 2095-9184 (print); ISSN 2095-9230 (online)
E-mail: jzus@zju.edu.cn

Event-triggered distributed cross-dimensional formation control for heterogeneous multi-agent systems*

Huimin WEI[†1], Chen PENG[†‡1], Min ZHAO[2]

[1]*School of Mechatronic Engineering and Automation, Shanghai University, Shanghai 200444, China*

[2]*School of Mathematics and Statistics, Nantong University, Nantong 226019, China*

[†]E-mail: weihuimin16@163.com; c.peng@shu.edu.cn

Received Sept. 15, 2023; Revision accepted Jan. 18, 2024; Crosschecked July 23, 2024

Abstract: This paper concerns the event-triggered distributed cross-dimensional formation control problem of heterogeneous multi-agent systems (HMASs) subject to limited network resources. The central aim is to design an effective distributed formation control scheme that will achieve the desired formation control objectives even in the presence of restricted communication. Consequently, a multi-dimensional HMAS is first developed, where a group of agents are assigned to several subgroups based on their dimensions. Then, to mitigate the excessive consumption of communication resources, a cross-dimensional event-triggered communication mechanism is designed to reduce the information interaction among agents with different dimensions. Under the proposed event-based communication mechanism, the problem of HMAS cross-dimensional formation control is transformed into the asymptotic stability problem of a closed-loop error system. Furthermore, several stability criteria for designing a cross-dimensional formation control protocol and communication schedule are presented in an environment where there is no information interaction among follower agents. Finally, a simulation case study is provided to validate the effectiveness of the proposed formation control protocol.

Key words: Heterogeneous multi-agent systems; Formation control; Cross-dimensional event-triggered mechanism
https://doi.org/10.1631/FITEE.2300627 **CLC number:** TP273

1 Introduction

In the realm of autonomous systems, the concept of formation control within multi-agent systems (MASs) has emerged as a captivating and transformative field of study (Weimerskirch et al., 2001; Oh et al., 2015; Rezaee and Abdollahi, 2015; Dou et al., 2020; Ning et al., 2023). Generally, MASs are composed of a collection of individual agents, ranging from robots (Yang Y et al., 2022) and drones (Dong et al., 2015) to autonomous vehicles (Ge et al., 2022, 2023, 2024; Xie et al., 2024), each possessing individual decision-making abilities and sensory capabilities. The primary objective of MAS formation control is to orchestrate and coordinate a group of agents so that they move and act collectively, and achieve predefined spatial configurations or formations. For this purpose, various formation control strategies, such as leader–follower control strategies, virtual-structure control strategies, and behavior-based control strategies, have been proposed for MASs by employing communication networks. It should be mentioned that most of the existing results (Weimerskirch et al., 2001; Dong et al., 2015; Oh et al., 2015; Rezaee and Abdollahi, 2015; Ge et al., 2022, 2023, 2024; Yang Y et al., 2022; Ning et al., 2023; Xie et al., 2024) are concerned with homogeneous agents. However, in practical scenarios, agents are

‡ Corresponding author

* Project supported by the National Natural Science Foundation of China (No. 62173218) and the International Cooperation Project of Shanghai Science and Technology Commission, China (No. 21190780300)

ORCID: Huimin WEI, https://orcid.org/0009-0008-9639-9365; Chen PENG, https://orcid.org/0000-0003-3652-2233

usually governed by non-identical kinetic equations. In this sense, heterogeneous systems are more applicable than homogeneous systems. Different from homogeneous systems, where all agents share similar characteristics, heterogeneous systems bring together a diverse ensemble of agents, each possessing unique capabilities, roles, and attributes. This diversity poses great challenges for cooperation among MASs.

In the context of heterogeneous multi-agent system (HMAS) formation control, the challenge lies in devising control algorithms that can seamlessly integrate agents with distinct kinematic and dynamic properties, sensing capabilities, and communication modalities. To handle this issue, concerted effort has been devoted to addressing the HMAS formation control challenge in recent years (Li et al., 2015; Meng et al., 2015). For example, the HMAS formation control problem was studied within the output regulation framework (Haghshenas et al., 2015), where the dynamics of leaders were identical. Jiang et al. (2019) investigated the linear HMAS distributed formation control problem when the state dimension and dynamics of leaders and followers were different. The HMAS time-varying formation control problem was solved using two event-triggered formation control schemes in Song et al. (2022). Note that most of the existing results related to HMAS formation control (Jiao et al., 2016; Ding and Zheng, 2017; Zhang D et al., 2018) involve different system matrices but identical system dimensions. In fact, the HMAS dynamics have different state dimensions. In Jiang et al. (2019), agents with different dimensions in an HMAS were divided into two groups (a leader group and a follower group) and the dimensions in each group were identical. However, in some special cases, such as the tracking tasks achieved by the cooperation of unmanned aerial vehicles and unmanned surface vehicles, follower agents have non-identical state dimensions, which leads to a requirement to achieve the desired formation in their own dimensions. In this context, the communication among agents with different dimensions will play a crucial role. Matrices were provided to achieve cross-dimensional information interaction among agents with different dimensions (Ma et al., 2022). It should be noted that too much information interaction among agents may lead to network congestion, especially in large-scale networked MASs. Thus, it is necessary to introduce event-triggered control to schedule inter-agent communication (Ju et al., 2022; Zhang XM et al., 2023). The event-triggered mechanisms in the existing literature involve agents with the same dimension even if they have different dynamics (Hu et al., 2017; Song et al., 2023), whereas, under the cluster consensus, agents are allocated in different groups to perform different tasks. The interactions among agents in the same group and agents in different groups should be inherently different. In this sense, Yang YP et al. (2024) designed sampled-data-based event-triggering mechanisms by incorporating intra-cluster and out-of-cluster communication. However, to the best of our knowledge, few studies related to event-triggered communication of cross-dimensional HMASs are available, which drives the current investigation.

This study focuses on the problem of distributed cross-dimensional formation control for an HMAS. The main contributions are twofold:

1. A complete HMAS is proposed where, compared with the partial HMAS developed in Ma et al. (2022), the agents in the same and different groups are all heterogeneous in the proposed HMAS.

2. A cross-dimensional event-triggered communication mechanism is designed, where the leader's information is included in the state response errors among the neighboring agents in both the same and different groups.

Notations: $\mathbb{R}^n$ and $\mathbb{R}^{m\times n}$ stand for the n-dimensional Euclidean space and $m\times n$ real matrix space, respectively. col$\{\cdot\}$ represents a column vector, diag$\{\cdot\}$ represents a diagonal matrix, and $\otimes$ denotes the Kronecker product for matrices. $\boldsymbol{P}\geq 0$ (or $\boldsymbol{P}>0$) indicates that $\boldsymbol{P}$ is positive semi-definite (or positive definite). $\mathbb{N}$ denotes the non-negative integer set. $\boldsymbol{I}_N$ and $\mathbf{0}_{M\times N}$ denote an N-dimensional identity matrix and an $M\times N$ matrix with all entries being zero, respectively.

2 Problem statement

2.1 Communication topology

Consider an MAS consisting of one leader and N followers. The information exchange among the N followers can be described by a digraph $\mathcal{G}=\{\mathcal{V},\mathcal{E},\boldsymbol{\mathcal{A}}\}$, where $\mathcal{V}=\{1,2,\ldots,N\}$ is the index set

of followers, $\mathcal{E}=\{(i,j):i,j\in\mathcal{V}\}$ stands for the edge set, and $\boldsymbol{\mathcal{A}}=[a_{ij}]_{N\times N}$ is the weighted adjacency matrix. Particularly, $a_{ij}=1$ if $(i,j)\in\mathcal{E}$ and $a_{ij}=0$ otherwise. In such a digraph $\mathcal{G}$, self-loops are excluded, i.e., $a_{ii}=0$. Define the Laplacian matrix of the digraph $\mathcal{G}$ as $\boldsymbol{\mathcal{L}}=[l_{ij}]_{N\times N}$, where $l_{ij}=-a_{ij}$ if $i\neq j$ and $l_{ij}=\sum_{j\neq i}a_{ij}$ otherwise. A directed path from follower j to follower i is a sequence of ordered edges $(j,j_1),(j_1,j_2),\ldots,(j_{p-1},j_p),(j_p,i)$, where $j_1,j_2,\ldots,j_p$ are distinct.

Let the leader be an additional node 0. Then the weighted adjacency matrix of the leader can be denoted as $\boldsymbol{M}=\mathrm{diag}\{m_1,m_2,\ldots,m_N\}$, where $m_i=1$ ($i\in\mathcal{V}$) if follower i can receive information from the leader and $m_i=0$ otherwise. Without loss of generality, we assume that there is a directed path from the leader to any follower in the digraph $\mathcal{G}$.

2.2 Cross-dimensional formation structures

In our work, we assume that followers can be divided into g ($1\leq g\leq N$) groups according to their state dimensions. In other words, agents with identical dimension are assigned in the same group. Correspondingly, the node index set $\mathcal{V}$ can be divided into g non-overlapping subsets, $\mathcal{V}_1,\mathcal{V}_2,\ldots,\mathcal{V}_g$. Furthermore, the following is given: $\mathcal{V}_j\neq\varnothing$ ($j=1,2,...,g$), $\bigcup_{j=1}^{g}\mathcal{V}_j=\mathcal{V}$, and $\mathcal{V}_j\bigcap\mathcal{V}_k=\varnothing$ ($\forall j,k\in\{1,2,...,g\}$ and $j\neq k$). In addition, subscripts $\bar{i}$ and $\bar{j}$ are introduced to represent subsets to which agents i and j belong, respectively. If $\bar{i}=\bar{j}$, the dimensions of agents i and j are the same, and the two agents i and j are in the same subgroup. Moreover, denote $n_{\bar{i}}$ as the dimension of state vectors and $m_{\bar{i}}$ as the number of agents in the $\bar{i}^{\mathrm{th}}$ subgroup. It is not difficult to see that $\sum_{\bar{i}=1}^{g}m_{\bar{i}}=N$. For the sake of simplicity, we assume that $\bar{i}\leq\bar{j}$ if $i<j$ ($\forall i,j\in\mathcal{V}$) and $n_{\bar{i}}<n_{\bar{j}}$ if $\bar{i}<\bar{j}$. Obviously, the state vector's dimension of agents in the g^{th} subgroup is higher than that of the ones in any other subgroups. It is also assumed that the leader's dimension is n_g, which means that the dimension of the leader is the highest.

2.3 Dynamics of HMASs

For the addressed cross-dimensional formation control issue, the dynamics of the leader agent are given as follows:

$$\begin{cases}\dot{\boldsymbol{x}}_0(t)=\boldsymbol{v}_0(t),\\ \dot{\boldsymbol{v}}_0(t)=\boldsymbol{A}_g\boldsymbol{x}_0(t)+\boldsymbol{B}_g\boldsymbol{v}_0(t),\end{cases}\tag{1}$$

where $\boldsymbol{x}_0(t)\in\mathbb{R}^{n_g}$ and $\boldsymbol{v}_0(t)\in\mathbb{R}^{n_g}$ are the position and velocity vectors respectively, and $\boldsymbol{A}_g\in\mathbb{R}^{n_g\times n_g}$ and $\boldsymbol{B}_g\in\mathbb{R}^{n_g\times n_g}$ are the coefficient matrices.

The dynamics of the i^{th} ($i\in\mathcal{V}$) follower are described by

$$\begin{cases}\dot{\boldsymbol{x}}_i(t)=\boldsymbol{v}_i(t),\\ \dot{\boldsymbol{v}}_i(t)=\boldsymbol{A}_i\boldsymbol{x}_i(t)+\boldsymbol{B}_i\boldsymbol{v}_i(t)+\boldsymbol{u}_i(t),\end{cases}\tag{2}$$

where $\boldsymbol{x}_i(t)\in\mathbb{R}^{n_{\bar{i}}}$ and $\boldsymbol{v}_i(t)\in\mathbb{R}^{n_{\bar{i}}}$ are the position and velocity vectors respectively, $\boldsymbol{u}_i(t)$ is the distributed control input vector, and $\boldsymbol{A}_i\in\mathbb{R}^{n_{\bar{i}}\times n_{\bar{i}}}$ and $\boldsymbol{B}_i\in\mathbb{R}^{n_{\bar{i}}\times n_{\bar{i}}}$ are the known real matrices.

Remark 1 Compared with the homogeneous MASs considered in Ma et al. (2022), the dynamics of followers (Eq. (2)) developed in our work are heterogeneous; that is, there are different system matrices, even if they are in the same subgroup. In other words, different agents have non-identical dynamics, so the addressed dynamical model is very general and more in line with reality.

Remark 2 We designed the subsequent cross-dimensional formation control protocol because higher-dimensional agents can receive global information from lower-dimensional agents, whereas agents with lower dimensions receive only partial information from higher-dimensional agents.

2.4 Cross-dimensional formation

To describe the cross-dimensional formation precisely, let us first introduce the following two matrices:

$$\boldsymbol{M}_{\bar{i}\bar{j}}=\begin{cases}\boldsymbol{I}_{n_{\bar{i}}}, & \bar{i}=\bar{j},\\ \begin{bmatrix}\boldsymbol{I}_{n_{\bar{i}}} & \boldsymbol{0}\end{bmatrix}_{n_{\bar{i}}\times n_{\bar{j}}}, & \bar{i}<\bar{j},\\ \begin{bmatrix}\boldsymbol{I}_{n_{\bar{j}}}\\ \boldsymbol{0}\end{bmatrix}_{n_{\bar{i}}\times n_{\bar{j}}}, & \bar{i}>\bar{j},\end{cases}\tag{3}$$

$$\boldsymbol{N}_{\bar{i}\bar{j}}=\begin{cases}\boldsymbol{I}_{n_{\bar{i}}}, & \bar{i}\leq\bar{j},\\ \begin{bmatrix}\boldsymbol{I}_{n_{\bar{j}}} & \boldsymbol{0}\\ \boldsymbol{0} & \boldsymbol{0}\end{bmatrix}_{n_{\bar{i}}\times n_{\bar{i}}}, & \bar{i}>\bar{j}.\end{cases}\tag{4}$$

Denote $\widehat{\boldsymbol{M}}_{\bar{i}\bar{j}}=\mathrm{diag}\{\boldsymbol{M}_{\bar{i}\bar{j}},\boldsymbol{M}_{\bar{i}\bar{j}}\}$ and $\widehat{\boldsymbol{N}}_{\bar{i}\bar{j}}=\mathrm{diag}\{\boldsymbol{N}_{\bar{i}\bar{j}},\boldsymbol{N}_{\bar{i}\bar{j}}\}$. According to Lemma 1 in Ma et al. (2022), we have

$$\widehat{\boldsymbol{N}}_{\bar{i}\bar{j}}\widehat{\boldsymbol{M}}_{\bar{i}g}=\widehat{\boldsymbol{M}}_{\bar{i}\bar{j}}\widehat{\boldsymbol{M}}_{\bar{j}g}.$$

Let $\boldsymbol{\zeta}_i(t)=[\boldsymbol{x}_i^{\mathrm{T}}(t),\ \boldsymbol{v}_i^{\mathrm{T}}(t)]^{\mathrm{T}}$ for $i\in\mathcal{V}$. It can be found that $\boldsymbol{\zeta}_0(t)\in\mathbb{R}^{2n_g}$ and $\boldsymbol{\zeta}_i(t)\in\mathbb{R}^{2n_{\bar{i}}}$ for

agent i ($i \in \mathcal{V}_i$). Define $\boldsymbol{f}_i(t) = [\boldsymbol{f}_{ix}^{\mathrm{T}}(t),\ \boldsymbol{f}_{iv}^{\mathrm{T}}(t)]^{\mathrm{T}}$ with $\boldsymbol{f}_{iv}(t) = \dot{\boldsymbol{f}}_{ix}(t)$ as the time-varying formation pattern of agent i. Then a definition of cross-dimensional formation of an HMAS consisting of Eqs. (1) and (2) is given as follows:

Definition 1 For any given bounded initial state, cross-dimensional formation is achieved if the following condition holds:

$$\lim_{t\to\infty}\left\{\boldsymbol{\zeta}_i(t) - \boldsymbol{f}_i(t) - \widehat{\boldsymbol{M}}_{\bar{i}g}\boldsymbol{\zeta}_0(t)\right\} = \boldsymbol{0},\ \forall i \in \mathcal{V}_i. \quad (5)$$

Remark 3 An illustrative example of the considered cross-dimensional formation of HMASs is provided in Fig. 1. Based on Definition 1, if condition (5) holds, it means that

$$\lim_{t\to\infty}\{\boldsymbol{\zeta}_i(t) - \boldsymbol{\zeta}_j(t) - (\boldsymbol{f}_i(t) - \boldsymbol{f}_j(t))\} = \boldsymbol{0}$$

for $i, j \in \mathcal{V}_{\bar{i}}$, which reduces to the formation formed by agents with the same dimension (Ge and Han, 2017). Furthermore, if $\left\{\boldsymbol{\zeta}_i(t) - \boldsymbol{f}_i(t) - \widehat{\boldsymbol{M}}_{\bar{i}g}\boldsymbol{\zeta}_0(t)\right\} \to \boldsymbol{0}$ as $t \to \infty$, we have

$$\begin{aligned}&\boldsymbol{N}_{\bar{i}\bar{j}}(\boldsymbol{\zeta}_i(t) - \boldsymbol{f}_i(t)) - \boldsymbol{M}_{\bar{i}\bar{j}}(\boldsymbol{\zeta}_j(t) - \boldsymbol{f}_j(t))\\ =\ &\boldsymbol{N}_{\bar{i}\bar{j}}(\boldsymbol{\zeta}_i(t) - \boldsymbol{f}_i(t)) - \boldsymbol{M}_{\bar{i}\bar{j}}(\boldsymbol{\zeta}_j(t) - \boldsymbol{f}_j(t))\\ &- \widehat{\boldsymbol{N}}_{\bar{i}\bar{j}}\widehat{\boldsymbol{M}}_{\bar{i}g}\boldsymbol{\zeta}_0(t) + \widehat{\boldsymbol{M}}_{\bar{i}\bar{j}}\widehat{\boldsymbol{M}}_{\bar{j}g}\boldsymbol{\zeta}_0(t)\end{aligned}$$

because of $\widehat{\boldsymbol{N}}_{\bar{i}\bar{j}}\widehat{\boldsymbol{M}}_{\bar{i}g} = \widehat{\boldsymbol{M}}_{\bar{i}\bar{j}}\widehat{\boldsymbol{M}}_{\bar{j}g}$. This further means

$$\begin{aligned}&\boldsymbol{N}_{\bar{i}\bar{j}}(\boldsymbol{\zeta}_i(t) - \boldsymbol{f}_i(t) - \boldsymbol{M}_{\bar{i}g}\boldsymbol{\zeta}_0(t))\\ -\ &\boldsymbol{M}_{\bar{i}\bar{j}}(\boldsymbol{\zeta}_j(t) - \boldsymbol{f}_j(t) - \widehat{\boldsymbol{M}}_{\bar{j}g}\boldsymbol{\zeta}_0(t)) \to \boldsymbol{0}\end{aligned}$$

for $i \in \mathcal{V}_{\bar{i}}, j \in \mathcal{V}_{\bar{j}}$ ($\bar{i} \neq \bar{j}$). In addition, from a mathematical perspective, the term $\widehat{\boldsymbol{M}}_{\bar{i}g}\boldsymbol{\zeta}_0(t)$ in condition (5) can be regarded as a projection of higher-dimensional vectors onto a lower-dimensional plane.

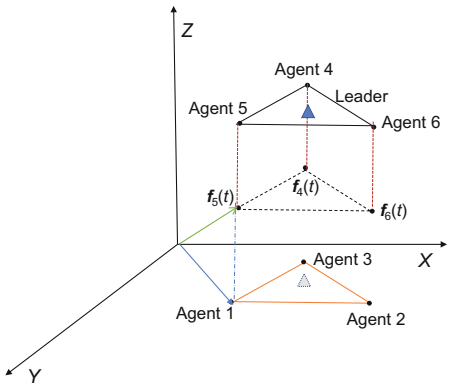

Fig. 1 Cross-dimensional formation of seven agents

Therefore, matrices (3) and (4) can be expressed as the information interactions among agents with different dimensions and thus have more theoretical significance.

2.5 Event-triggering mechanisms

In our work, an event-based data transmission scheme is exploited to mitigate the excessive consumption of communication resources, as shown in Fig. 2. Now, let us show such a scheme.

Denote $t_k^i h$ as the k^{th} event release instant of the i^{th} agent. Then the event-triggering time sequence can be described as $\{t_0^i h, t_1^i h, \ldots, t_k^i h, \ldots\}$ with $t_k^i \in \mathbb{N}$, $k \in \mathbb{N}$, and $t_0^i h = 0$. The next event-triggering instant of the i^{th} agent can be calculated as

$$t_{k+1}^i h = t_k^i h + \{\vartheta h | \hbar_i(t_k^i h + \vartheta h) > 0\}, \quad (6)$$

where the event function is selected as

$$\hbar_i(t_k^i h + \vartheta h) = \boldsymbol{e}_i^{\mathrm{T}}(t_k^i h + \vartheta h)\boldsymbol{\Phi}_i\boldsymbol{e}_i(t_k^i h + \vartheta h) - \Upsilon,$$

with the weighting matrix $\boldsymbol{\Phi}_i > 0$, the measurement error between the last event-triggered data and the current data

$$\begin{aligned}&\boldsymbol{e}_i(t_k^i h + \vartheta h)\\ =&\boldsymbol{\zeta}_i(t_k^i h + \vartheta h) - \boldsymbol{f}_i(t_k^i h + \vartheta h) - \left(\boldsymbol{\zeta}_i(t_k^i h) - \boldsymbol{f}_i(t_k^i h)\right),\end{aligned} \quad (7)$$

and the threshold-related parameter

$$\begin{aligned}\Upsilon = &\sum_{j\in\mathcal{V}_i}\sigma_{j\bar{i}}\boldsymbol{\rho}_j^{\mathrm{T}}(t_k^i h)\boldsymbol{\Omega}_{j\bar{i}}\boldsymbol{\rho}_j(t_k^i h)\\ &+ \sum_{\bar{j}=1,\bar{j}\neq\bar{i}}^{g}\sum_{j\in\mathcal{V}_j}\sigma_{j\bar{j}}\hat{\boldsymbol{\rho}}_j^{\mathrm{T}}(t_{k_j'}^i h)\boldsymbol{\Omega}_{j\bar{j}}\hat{\boldsymbol{\rho}}_j(t_{k_j'}^i h).\end{aligned}$$

Here, $\boldsymbol{\Omega}_{j\bar{i}} > 0$ and $\boldsymbol{\Omega}_{j\bar{j}} > 0$ are the designed weighting matrices, $\sigma_{j\bar{i}}, \sigma_{j\bar{j}} \in (0, 1)$ are the threshold parameters to be given, and $\boldsymbol{\rho}(t_k^i h)$ denotes the state error between agent i and its neighbors in the same subgroup at $t_k^i h$ with the following form:

$$\begin{aligned}&\boldsymbol{\rho}_j(t_k^i h)\\ =&a_{ij}\left(\boldsymbol{\zeta}_i(t_k^i h) - \boldsymbol{f}_i(t_k^i h) - \left(\boldsymbol{\zeta}_j\left(t_{k_j'}^i h\right) - \boldsymbol{f}_j\left(t_{k_j'}^i h\right)\right)\right)\\ &+ m_i\left(\boldsymbol{\zeta}_i(t_k^i h) - \boldsymbol{f}_i(t_k^i h) - \widehat{\boldsymbol{M}}_{\bar{i}g}\boldsymbol{\zeta}_0(t_k^i h)\right).\end{aligned} \quad (8)$$

However, when the dimensions of agent i and its neighbors are different, the corresponding state error

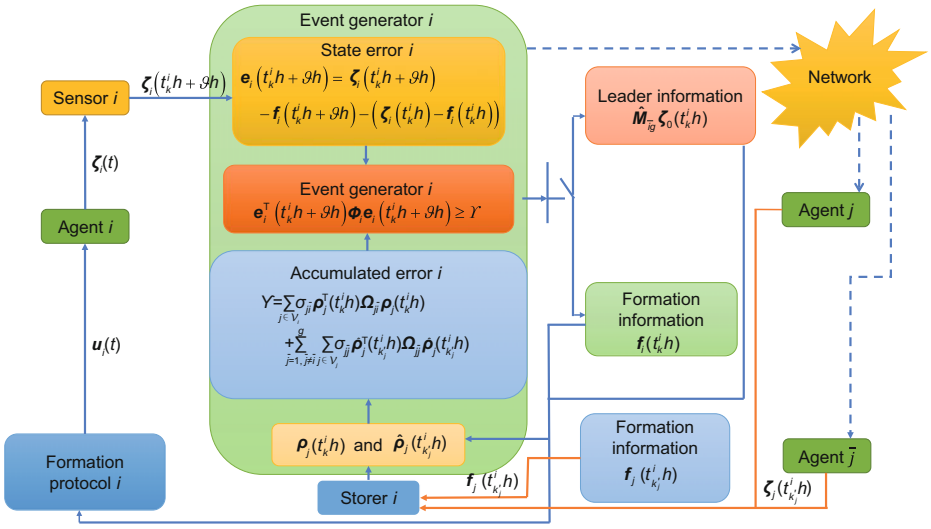

Fig. 2 Event-triggered distributed formation control for agent i

at $t_k^i h$ is given by

$$\begin{aligned}\hat{\boldsymbol{\rho}}\left(t_{k_j'}^i h\right) =& a_{ij}\Bigg(-\widehat{\boldsymbol{M}}_{\bar{i}\bar{j}}\left(\boldsymbol{\zeta}_j\left(t_{k_j'}^i h\right)-\boldsymbol{f}_j\left(t_{k_j'}^i h\right)\right)\\ &+\widehat{\boldsymbol{N}}_{\bar{i}\bar{j}}\left(\boldsymbol{\zeta}_i(t_k^i h)-\boldsymbol{f}_i(t_k^i h)\right)\Bigg)+m_i\left(\boldsymbol{\zeta}_i(t_k^i h)\right.\\ &\left.-\boldsymbol{f}_i(t_k^i h)-\widehat{\boldsymbol{M}}_{\bar{i}g}\boldsymbol{\zeta}_0(t_k^i h)\right).\end{aligned}$$

Remark 4 Note that compared with the IIC-SDETM (Eq. (5) in Yang YP et al. (2024)), the term containing leader's information in Eq. (8), $m_i\left(\boldsymbol{\zeta}_i(t_k^i h)-\boldsymbol{f}_i(t_k^i h)-\widehat{\boldsymbol{M}}_{\bar{i}g}\boldsymbol{\zeta}_0(t_k^i h)\right)$, is added in our work. This term can be considered as the disagreement vector between the i^{th} agent and the leader at $t_k^i h$. If $\lim_{t\to\infty}\left\{\boldsymbol{\zeta}_i(t)-\boldsymbol{f}_i(t)-\widehat{\boldsymbol{M}}_{\bar{i}g}\boldsymbol{\zeta}_0(t)\right\}=\boldsymbol{0}$, the control tasks are said to be achieved. This term is also considered in some existing works on the event-triggered control strategies for MASs (Zhao et al., 2018; Xia et al., 2023). Moreover, the introduction of this term effectively avoids the fact that $\boldsymbol{\Lambda}\boldsymbol{\mathcal{E}}_{25}^{\mathrm{T}}\widetilde{\boldsymbol{L}}^{\mathrm{T}}\boldsymbol{\Omega}\widetilde{\boldsymbol{L}}\boldsymbol{\mathcal{E}}_{25}$ cannot be calculated due to the irreversibility of $\widetilde{\boldsymbol{L}}$. Also, the dimensions of all agents in Yang YP et al. (2024) are identical, while those in this study are not exactly the same.

2.6 Control protocol

In this subsection, a distributed formation control protocol is developed as follows:

$$\begin{aligned}\boldsymbol{u}_i(t)=\boldsymbol{c}_i(t)+\boldsymbol{K}_i\Bigg(&\sum_{j\in\mathcal{V}_i}a_{ij}\Bigg(\widehat{\boldsymbol{N}}_{\bar{i}\bar{j}}\left(\boldsymbol{\zeta}_i(t_k^i h)-\boldsymbol{f}_i(t_k^i h)\right)\\ &-\widehat{\boldsymbol{M}}_{\bar{i}\bar{j}}\left(\boldsymbol{\zeta}_j\left(t_{k_j'}^i h\right)-\boldsymbol{f}_j\left(t_{k_j'}^i h\right)\right)\Bigg)\\ &+m_i\left(\boldsymbol{\zeta}_i(t_k^i h)-\boldsymbol{f}_i(t_k^i h)-\widehat{\boldsymbol{M}}_{\bar{i}g}\boldsymbol{\zeta}_0(t_k^i h)\right)\Bigg),\end{aligned}\tag{9}$$

where $t\in[t_k^i h, t_{k+1}^i h)$ for $i\in\mathcal{V}_i$, $\boldsymbol{\zeta}_j\left(t_{k_j'}^i h\right)$ is the latest transmitted measurement of the neighbor of agent i with

$$t_{k_j'}^i h=\arg\min_{k_j'}\left\{lh-t_{k_j'}^i h|l>t_{k_j'}^i, t_{k_j'}^i\in\mathbb{N}\right\},$$

$\boldsymbol{K}_i$ stands for a gain matrix to be designed, and $\boldsymbol{c}_i(t)=\dot{\boldsymbol{f}}_{iv}(t)-[\boldsymbol{A}_i,\ \boldsymbol{B}_i]\boldsymbol{f}_i(t)$ is the formation compensation signal vector determined by $\boldsymbol{f}_i(t)$ with $\boldsymbol{f}_{iv}(t)$ being differentially derivable.

Substituting the above designed controller (9) into agent i's dynamics, we have

$$\begin{aligned}\dot{\boldsymbol{\zeta}}_i(t)=&\boldsymbol{G}_i\boldsymbol{\zeta}_i(t)+\boldsymbol{H}_{\bar{i}}\boldsymbol{c}_i(t)\\ &+\boldsymbol{H}_{\bar{i}}\boldsymbol{K}_i\Bigg(\sum_{j\in\mathcal{V}_i}a_{ij}\Bigg(\widehat{\boldsymbol{N}}_{\bar{i}\bar{j}}\left(\boldsymbol{\zeta}_i(t_k^i h)-\boldsymbol{f}_i(t_k^i h)\right)\\ &-\widehat{\boldsymbol{M}}_{\bar{i}\bar{j}}\left(\boldsymbol{\zeta}_j\left(t_{k_j'}^i h\right)-\boldsymbol{f}_j\left(t_{k_j'}^i h\right)\right)\Bigg)\\ &+m_i\left(\boldsymbol{\zeta}_i(t_k^i h)-\boldsymbol{f}_i(t_k^i h)-\widehat{\boldsymbol{M}}_{\bar{i}g}\boldsymbol{\zeta}_0(t_k^i h)\right)\Bigg).\end{aligned}\tag{10}$$

In addition, the leader's dynamics (1) can be rewritten as follows:

$$\dot{\boldsymbol{\zeta}}_0(t)=\boldsymbol{G}_0\boldsymbol{\zeta}_0(t),\tag{11}$$

where

$$\boldsymbol{G}_i=\begin{bmatrix}\boldsymbol{0}_{n_{\bar{i}}\times n_{\bar{i}}} & \boldsymbol{I}_{n_{\bar{i}}}\\ \boldsymbol{A}_i & \boldsymbol{B}_i\end{bmatrix},\ \boldsymbol{H}_{\bar{i}}=\begin{bmatrix}\boldsymbol{0}_{n_{\bar{i}}\times n_{\bar{i}}}\\ \boldsymbol{I}_{n_{\bar{i}}}\end{bmatrix},$$

for $i=0,1,\ldots,N$ and $\bar{i}=1,2,\ldots,g$.

Letting

$$\boldsymbol{\theta}_i(t)=\boldsymbol{\zeta}_i(t)-\boldsymbol{f}_i(t)-\widehat{\boldsymbol{M}}_{\bar{i}g}\boldsymbol{\zeta}_0(t),$$

we have

$$\begin{aligned}\dot{\boldsymbol{\theta}}_i(t)=&\boldsymbol{G}_i\boldsymbol{\theta}_i(t)+\boldsymbol{H}_{\bar{i}}\boldsymbol{K}_i\Bigg(\sum_{j\in\mathcal{V}_i}a_{ij}\Big(\boldsymbol{N}_{\bar{i}\bar{j}}\boldsymbol{\theta}_i(t_k^ih)\\&-\boldsymbol{M}_{\bar{i}\bar{j}}\boldsymbol{\theta}_i\left(t_{k_j'}^ih\right)\Big)+m_i\boldsymbol{\theta}_i(t_k^ih)\Bigg).\end{aligned}\tag{12}$$

In what follows, define $\ell_k^ih=t_k^ih+\vartheta h$ with $\vartheta\in\{0,1,...,t_{k+1}^i-t_k^i-1\}$ and $\boldsymbol{e}_i(t_k^ih+\vartheta h)=\boldsymbol{\zeta}_i(t_k^ih+\vartheta h)-\boldsymbol{f}_i(t_k^ih+\vartheta h)-(\boldsymbol{\zeta}_i(t_k^ih)-\boldsymbol{f}_i(t_k^ih))$. The dynamics (12) can be reconstructed as

$$\begin{aligned}\dot{\boldsymbol{\theta}}_i(t)=&\boldsymbol{G}_i\boldsymbol{\theta}_i(t)+\boldsymbol{H}_{\bar{i}}\boldsymbol{K}_i\Bigg(\sum_{j\in\mathcal{V}_i}a_{ij}\Big(\widehat{\boldsymbol{N}}_{\bar{i}\bar{j}}(\boldsymbol{\theta}_i(\ell_k^ih)\\&-\boldsymbol{e}_i(\ell_k^ih))-\widehat{\boldsymbol{M}}_{\bar{i}\bar{j}}\left(\boldsymbol{\theta}_j(\ell_k^ih)-\boldsymbol{e}_j(\ell_k^ih)\right)\Big)\\&+m_i\left(\boldsymbol{\theta}_i(\ell_k^ih)-\boldsymbol{e}_i(\ell_k^ih)\right)\Bigg).\end{aligned}\tag{13}$$

Introduce an artificial time delay $\tau(t)=t-\ell_k^ih$. Obviously, $\tau(t)$ is a discontinuous function satisfying $\tau_{\mathrm{m}}\le\tau(t)\le\tau_{\mathrm{M}}+h$, where τ_{M} and τ_{m} are the upper and lower bounds of time delay $\tau(t)$, respectively. Therefore, one can express Eq. (13) as

$$\begin{aligned}\dot{\boldsymbol{\theta}}_i(t)=&\boldsymbol{G}_i\boldsymbol{\theta}_i(t)+\boldsymbol{H}_{\bar{i}}\boldsymbol{K}_i\Bigg(\sum_{j\in\mathcal{V}_i}a_{ij}\big(\widehat{\boldsymbol{N}}_{\bar{i}\bar{j}}(\boldsymbol{\theta}_i(t-\tau(t))\\&-\boldsymbol{e}_i(t-\tau(t)))-\widehat{\boldsymbol{M}}_{\bar{i}\bar{j}}(\boldsymbol{\theta}_j(t-\tau(t))\\&-\boldsymbol{e}_j(t-\tau(t)))\big)+m_i(\boldsymbol{\theta}_i(t-\tau(t))\\&-\boldsymbol{e}_i(t-\tau(t)))\Bigg).\end{aligned}\tag{14}$$

For the sake of simplicity, define

$$\begin{aligned}\boldsymbol{\theta}(t)=&\left[\boldsymbol{\theta}_1^{\mathrm{T}}(t),\ \boldsymbol{\theta}_2^{\mathrm{T}}(t),\ ...,\ \boldsymbol{\theta}_N^{\mathrm{T}}(t)\right]^{\mathrm{T}},\\\boldsymbol{e}(t-\tau(t))=&\left[\boldsymbol{e}_1^{\mathrm{T}}(t-\tau(t)),\ \boldsymbol{e}_2^{\mathrm{T}}(t-\tau(t)),\right.\\&\left.\ ...,\ \boldsymbol{e}_N^{\mathrm{T}}(t-\tau(t))\right]^{\mathrm{T}}.\end{aligned}$$

$\widetilde{\boldsymbol{L}}$ is defined as an $N\times N$ block matrix where its $(i,j)^{\mathrm{th}}$ block is $\sum_{j=1}^N a_{ij}\boldsymbol{N}_{\bar{i}\bar{j}}$ if $i=j$ and $-a_{ij}\boldsymbol{M}_{\bar{i}\bar{j}}$ otherwise (Ma et al., 2022). The following closed-loop error system can be obtained:

$$\begin{aligned}\dot{\boldsymbol{\theta}}(t)=&\boldsymbol{G}\boldsymbol{\theta}(t)+\boldsymbol{H}\boldsymbol{K}\widetilde{\boldsymbol{D}}\boldsymbol{\theta}(t-\tau(t))\\&-\boldsymbol{H}\boldsymbol{K}\widetilde{\boldsymbol{D}}\boldsymbol{e}(t-\tau(t)),\end{aligned}\tag{15}$$

where

$$\begin{cases}\boldsymbol{G}=\mathrm{diag}\{\boldsymbol{G}_1,\boldsymbol{G}_2,\ldots,\boldsymbol{G}_N\},\\\boldsymbol{H}=\mathrm{diag}\{\boldsymbol{I}_{m_1}\otimes\boldsymbol{H}_1,\boldsymbol{I}_{m_2}\otimes\boldsymbol{H}_2,\ldots,\boldsymbol{I}_{m_g}\otimes\boldsymbol{H}_g\},\\\boldsymbol{K}=\mathrm{diag}\{\boldsymbol{K}_1,\boldsymbol{K}_2,\ldots,\boldsymbol{K}_N\},\\\widetilde{\boldsymbol{M}}=\mathrm{diag}\{m_1\boldsymbol{I}_{2n_{\bar{1}}},m_2\boldsymbol{I}_{2n_{\bar{2}}},\ldots,m_g\boldsymbol{I}_{2n_g}\},\\\widetilde{\boldsymbol{D}}=\widetilde{\boldsymbol{L}}+\widetilde{\boldsymbol{M}}.\end{cases}$$

3 Main results

In this section, some sufficient criteria are presented for asymptotic stability of the resulting closed-loop error system (15) under the proposed cross-dimensional event-triggered communication protocol (9). First, consider the following Lyapunov–Krasovskii functional (LKF):

$$\begin{aligned}V(t,\boldsymbol{\theta},\dot{\boldsymbol{\theta}})=&\boldsymbol{\theta}^{\mathrm{T}}(t)\boldsymbol{P}\boldsymbol{\theta}(t)+\int_{t-\tau_{\mathrm{m}}}^{t}\boldsymbol{\theta}^{\mathrm{T}}(s)\boldsymbol{Q}_1\boldsymbol{\theta}(s)\mathrm{d}s\\&+\int_{t-\tau_{\mathrm{M}}}^{t-\tau_{\mathrm{m}}}\boldsymbol{\theta}^{\mathrm{T}}(s)\boldsymbol{Q}_2\boldsymbol{\theta}(s)\mathrm{d}s\\&+\tau_{\mathrm{m}}\int_{-\tau_{\mathrm{m}}}^{0}\int_{t+\theta}^{t}\dot{\boldsymbol{\theta}}^{\mathrm{T}}(s)\boldsymbol{R}_1\dot{\boldsymbol{\theta}}(s)\mathrm{d}s\mathrm{d}\boldsymbol{\theta}\\&+\delta\int_{-\tau_{\mathrm{M}}}^{-\tau_{\mathrm{m}}}\int_{t+\theta}^{t}\dot{\boldsymbol{\theta}}^{\mathrm{T}}(s)\boldsymbol{R}_2\dot{\boldsymbol{\theta}}(s)\mathrm{d}s\mathrm{d}\boldsymbol{\theta},\end{aligned}\tag{16}$$

where

$$\begin{cases}\boldsymbol{P}=\mathrm{diag}\{\boldsymbol{P}_1,\boldsymbol{P}_2,\ldots,\boldsymbol{P}_N\},\\\boldsymbol{Q}_1=\mathrm{diag}\{\boldsymbol{Q}_{11},\boldsymbol{Q}_{12},\ldots,\boldsymbol{Q}_{1N}\},\\\boldsymbol{Q}_2=\mathrm{diag}\{\boldsymbol{Q}_{21},\boldsymbol{Q}_{22},\ldots,\boldsymbol{Q}_{2N}\},\\\boldsymbol{R}_1=\mathrm{diag}\{\boldsymbol{R}_{11},\boldsymbol{R}_{12},\ldots,\boldsymbol{R}_{1N}\},\\\boldsymbol{R}_2=\mathrm{diag}\{\boldsymbol{R}_{21},\boldsymbol{R}_{22},\ldots,\boldsymbol{R}_{2N}\},\end{cases}$$

with $\boldsymbol{P}_i>0$, $\boldsymbol{Q}_{ai}>0$, $\boldsymbol{R}_{ai}>0$ for $a=1,2$, $i=1,2,...,N$, and $\delta=\tau_{\mathrm{M}}-\tau_{\mathrm{m}}$.

Theorem 1 For given scalars $\sigma_i\in[0,1)$, τ_{m}, τ_{M}, and $\rho_a>0$, the resulting closed-loop error system (15) under the proposed cross-dimensional event-triggered communication protocol (9) is asymptotically stable, if there are real matrices $\hat{\boldsymbol{P}}_i=\hat{\boldsymbol{P}}_i^{\mathrm{T}}>0$, $\hat{\boldsymbol{Q}}_{ai}=\hat{\boldsymbol{Q}}_{ai}^{\mathrm{T}}>0$, $\hat{\boldsymbol{R}}_{ai}=\hat{\boldsymbol{R}}_{ai}^{\mathrm{T}}>0$,

$\hat{\boldsymbol{\Phi}}_i=\hat{\boldsymbol{\Phi}}_i^{\mathrm{T}}>0$, $\hat{\boldsymbol{\Omega}}_i=\hat{\boldsymbol{\Omega}}_i^{\mathrm{T}}>0$, $\hat{\boldsymbol{S}}_i$, and $\hat{\boldsymbol{K}}_i$ ($i\in\mathcal{V}$ and $a=1,2$) with appropriate dimensions such that

$$\begin{bmatrix}\hat{\boldsymbol{R}}_2 & \hat{\boldsymbol{S}}\\ \hat{\boldsymbol{S}}^{\mathrm{T}} & \hat{\boldsymbol{R}}_2\end{bmatrix}>0, \tag{17}$$

$$\begin{bmatrix}\hat{\boldsymbol{\Theta}} & \tau_{\mathrm{m}}\hat{\boldsymbol{\Gamma}}^{\mathrm{T}} & \delta\hat{\boldsymbol{\Gamma}}^{\mathrm{T}}\\ * & -2\rho_1\hat{\boldsymbol{P}}+\rho_1^2\hat{\boldsymbol{R}}_1 & \boldsymbol{0}\\ * & * & -2\rho_2\hat{\boldsymbol{P}}+\rho_2^2\hat{\boldsymbol{R}}_2\end{bmatrix}<0, \tag{18}$$

where

$$\begin{aligned}\hat{\boldsymbol{\Theta}}=&\boldsymbol{\mathcal{E}}_1^{\mathrm{T}}\big(\boldsymbol{G}\hat{\boldsymbol{P}}\boldsymbol{\mathcal{E}}_1+\boldsymbol{H}\hat{\boldsymbol{K}}\boldsymbol{\mathcal{E}}_2-\boldsymbol{H}\hat{\boldsymbol{K}}\boldsymbol{\mathcal{E}}_5\big)\\&+\big(\boldsymbol{G}\hat{\boldsymbol{P}}\boldsymbol{\mathcal{E}}_1+\boldsymbol{H}\hat{\boldsymbol{K}}\boldsymbol{\mathcal{E}}_2-\boldsymbol{H}\hat{\boldsymbol{K}}\boldsymbol{\mathcal{E}}_5\big)^{\mathrm{T}}\boldsymbol{\mathcal{E}}_1\\&+\boldsymbol{\mathcal{E}}_1^{\mathrm{T}}\hat{\boldsymbol{Q}}_1\boldsymbol{\mathcal{E}}_1-\boldsymbol{\mathcal{E}}_3^{\mathrm{T}}(\hat{\boldsymbol{Q}}_1-\hat{\boldsymbol{Q}}_2)\boldsymbol{\mathcal{E}}_3-\boldsymbol{\mathcal{E}}_4^{\mathrm{T}}\hat{\boldsymbol{Q}}_2\boldsymbol{\mathcal{E}}_4\\&+\boldsymbol{\mathcal{E}}_{13}^{\mathrm{T}}\hat{\boldsymbol{R}}_1\boldsymbol{\mathcal{E}}_{13}-\boldsymbol{\mathcal{E}}_5^{\mathrm{T}}\hat{\boldsymbol{\Phi}}\boldsymbol{\mathcal{E}}_5+\boldsymbol{\Lambda}\boldsymbol{\mathcal{E}}_{25}^{\mathrm{T}}\hat{\boldsymbol{\Omega}}\boldsymbol{\mathcal{E}}_{25}\\&-\begin{bmatrix}\boldsymbol{\mathcal{E}}_{24}\\ \boldsymbol{\mathcal{E}}_{32}\end{bmatrix}^{\mathrm{T}}\begin{bmatrix}\hat{\boldsymbol{R}}_2 & \hat{\boldsymbol{S}}\\ \hat{\boldsymbol{S}}^{\mathrm{T}} & \hat{\boldsymbol{R}}_2\end{bmatrix}\begin{bmatrix}\boldsymbol{\mathcal{E}}_{24}\\ \boldsymbol{\mathcal{E}}_{32}\end{bmatrix},\\ \hat{\boldsymbol{\Gamma}}=&[\hat{\boldsymbol{P}}\boldsymbol{G},\ \ \boldsymbol{H}\hat{\boldsymbol{K}},\ \ \boldsymbol{0},\ \ \boldsymbol{0},\ \ -\boldsymbol{H}\hat{\boldsymbol{K}}],\end{aligned}$$

with $\hat{\boldsymbol{P}}=\mathrm{diag}\{\hat{\boldsymbol{P}}_i\}_N$, $\hat{\boldsymbol{Q}}_a=\mathrm{diag}\{\hat{\boldsymbol{Q}}_{ai}\}_N$, $\hat{\boldsymbol{R}}_a=\mathrm{diag}\{\hat{\boldsymbol{R}}_{ai}\}_N$, $\hat{\boldsymbol{S}}=\mathrm{diag}\{\hat{\boldsymbol{S}}_i\}_N$, and $\boldsymbol{\Lambda}=\mathrm{diag}\{\sigma_i\}_N$. Moreover, the formation gain matrices and event-triggered weighting matrices can be calculated as

$$\begin{aligned}\boldsymbol{K}=&\hat{\boldsymbol{K}}\widetilde{\boldsymbol{D}}^{-1}\hat{\boldsymbol{P}}^{-1},\ \boldsymbol{\Phi}=\hat{\boldsymbol{P}}^{-1}\hat{\boldsymbol{\Phi}}\hat{\boldsymbol{P}}^{-1},\\ \boldsymbol{\Omega}=&(\widetilde{\boldsymbol{D}}^{\mathrm{T}})^{-1}\hat{\boldsymbol{P}}^{-1}\hat{\boldsymbol{\Omega}}\hat{\boldsymbol{P}}^{-1}\widetilde{\boldsymbol{D}}^{\mathrm{T}}.\end{aligned} \tag{19}$$

Proof Define $\boldsymbol{\xi}(t)=\mathrm{col}\{\boldsymbol{\theta}(t),\boldsymbol{\theta}(t-\tau(t)),\boldsymbol{\theta}(t-\tau_{\mathrm{m}}),\boldsymbol{\theta}(t-\tau_{\mathrm{M}}),\boldsymbol{e}(t-\tau(t))\}$ and let $\boldsymbol{\mathcal{E}}_{ij}=\boldsymbol{\mathcal{E}}_i-\boldsymbol{\mathcal{E}}_j$ where $\boldsymbol{\mathcal{E}}_i$ represents the i^{th} row elements of $10n_x\times 10n_x$ identity matrix with n_x being the dimension of the position/velocity vector of the MASs (2) satisfying $n_x=\sum_{\bar{i}=1}^{g}m_{\bar{i}}n_{\bar{i}}$. In what follows, taking the time derivative of $V(t,\boldsymbol{\theta},\dot{\boldsymbol{\theta}})$ yields

$$\begin{aligned}&\dot{V}(t,\boldsymbol{\theta},\dot{\boldsymbol{\theta}})\\=&\boldsymbol{\xi}^{\mathrm{T}}(t)\boldsymbol{\mathcal{E}}_1^{\mathrm{T}}\Big(\boldsymbol{PG}\boldsymbol{\mathcal{E}}_1+\boldsymbol{HPK}\widetilde{\boldsymbol{D}}\boldsymbol{\mathcal{E}}_2-\boldsymbol{HPK}\widetilde{\boldsymbol{D}}\boldsymbol{\mathcal{E}}_5\Big)\boldsymbol{\xi}(t)\\&+\boldsymbol{\xi}^{\mathrm{T}}(t)\Big(\boldsymbol{PG}\boldsymbol{\mathcal{E}}_1+\boldsymbol{HPK}\widetilde{\boldsymbol{D}}\boldsymbol{\mathcal{E}}_2-\boldsymbol{HPK}\widetilde{\boldsymbol{D}}\boldsymbol{\mathcal{E}}_5\Big)^{\mathrm{T}}\boldsymbol{\mathcal{E}}_1\boldsymbol{\xi}(t)\\&+\boldsymbol{\xi}^{\mathrm{T}}(t)\Big(\boldsymbol{\mathcal{E}}_1^{\mathrm{T}}\boldsymbol{Q}_1\boldsymbol{\mathcal{E}}_1-\boldsymbol{\mathcal{E}}_3^{\mathrm{T}}(\boldsymbol{Q}_1-\boldsymbol{Q}_2)\boldsymbol{\mathcal{E}}_3-\boldsymbol{\mathcal{E}}_4^{\mathrm{T}}\boldsymbol{Q}_2\boldsymbol{\mathcal{E}}_4\Big)\boldsymbol{\xi}(t)\\&+\dot{\boldsymbol{\theta}}^{\mathrm{T}}(t)\Big(\tau_{\mathrm{m}}^2\boldsymbol{R}_1+\delta^2\boldsymbol{R}_2\Big)\dot{\boldsymbol{\theta}}(t)-\tau_{\mathrm{m}}\int_{-\tau_{\mathrm{m}}}^{0}\dot{\boldsymbol{\theta}}^{\mathrm{T}}(s)\boldsymbol{R}_1\dot{\boldsymbol{\theta}}(s)\mathrm{d}s\\&-\delta\int_{t-\tau_{\mathrm{M}}}^{t-\tau_{\mathrm{m}}}\dot{\boldsymbol{\theta}}^{\mathrm{T}}(s)\boldsymbol{R}_2\dot{\boldsymbol{\theta}}(s)\mathrm{d}s.\end{aligned} \tag{20}$$

By virtue of Jensen's inequality, we have

$$-\tau_{\mathrm{m}}\int_{-\tau_{\mathrm{m}}}^{0}\dot{\boldsymbol{\theta}}^{\mathrm{T}}(s)\boldsymbol{R}_1\dot{\boldsymbol{\theta}}(s)\mathrm{d}s\le\boldsymbol{\xi}^{\mathrm{T}}(t)\boldsymbol{\mathcal{E}}_{13}^{\mathrm{T}}\boldsymbol{R}_1\boldsymbol{\mathcal{E}}_{13}\boldsymbol{\xi}(t). \tag{21}$$

Applying Lemma 1 in Ge and Han (2015) renders

$$\begin{aligned}&-\delta\int_{t-\tau_{\mathrm{M}}}^{t-\tau_{\mathrm{m}}}\dot{\boldsymbol{\theta}}^{\mathrm{T}}(s)\boldsymbol{R}_2\dot{\boldsymbol{\theta}}(s)\mathrm{d}s\\\le&-\boldsymbol{\xi}^{\mathrm{T}}(t)\begin{bmatrix}\boldsymbol{\mathcal{E}}_{24}\\ \boldsymbol{\mathcal{E}}_{32}\end{bmatrix}^{\mathrm{T}}\begin{bmatrix}\boldsymbol{R}_2 & \boldsymbol{S}\\ \boldsymbol{S}^{\mathrm{T}} & \boldsymbol{R}_2\end{bmatrix}\begin{bmatrix}\boldsymbol{\mathcal{E}}_{24}\\ \boldsymbol{\mathcal{E}}_{32}\end{bmatrix}\boldsymbol{\xi}(t),\end{aligned} \tag{22}$$

where $\boldsymbol{S}$ is a real matrix with appropriate dimension satisfying

$$\begin{bmatrix}\boldsymbol{R}_2 & \boldsymbol{S}\\ \boldsymbol{S}^{\mathrm{T}} & \boldsymbol{R}_2\end{bmatrix}>0. \tag{23}$$

Moreover, it follows from Eq. (7) that

$$\begin{aligned}&\boldsymbol{e}^{\mathrm{T}}(t-\tau(t))\boldsymbol{\Phi}\boldsymbol{e}(t-\tau(t))\\\le&\boldsymbol{\Lambda}\boldsymbol{\xi}^{\mathrm{T}}(t)\boldsymbol{\mathcal{E}}_{25}^{\mathrm{T}}\widetilde{\boldsymbol{D}}^{\mathrm{T}}\boldsymbol{\Omega}\widetilde{\boldsymbol{D}}\boldsymbol{\mathcal{E}}_{25}\boldsymbol{\xi}(t),\end{aligned} \tag{24}$$

where

$$\begin{cases}\boldsymbol{\Phi}=\mathrm{diag}\{\boldsymbol{\Phi}_1,\boldsymbol{\Phi}_2,\dots,\boldsymbol{\Phi}_N\},\\ \boldsymbol{\Omega}=\mathrm{diag}\{\boldsymbol{\Omega}_1,\boldsymbol{\Omega}_2,\dots,\boldsymbol{\Omega}_N\},\\ \boldsymbol{\Lambda}=\mathrm{diag}\{\sigma_1,\sigma_2,\dots,\sigma_N\}.\end{cases}$$

Combining expressions (20)–(24) leads to

$$\dot{V}(t,\boldsymbol{\theta},\dot{\boldsymbol{\theta}})\le\boldsymbol{\xi}^{\mathrm{T}}(t)\Big(\boldsymbol{\Theta}+\boldsymbol{\Gamma}^{\mathrm{T}}(\tau_{\mathrm{m}}^2\boldsymbol{R}_1+\delta^2\boldsymbol{R}_2)\boldsymbol{\Gamma}\Big)\boldsymbol{\xi}(t), \tag{25}$$

where

$$\begin{aligned}\boldsymbol{\Theta}=&\boldsymbol{\mathcal{E}}_1^{\mathrm{T}}\Big(\boldsymbol{PG}\boldsymbol{\mathcal{E}}_1+\boldsymbol{HPK}\widetilde{\boldsymbol{D}}\boldsymbol{\mathcal{E}}_2-\boldsymbol{HPK}\widetilde{\boldsymbol{D}}\boldsymbol{\mathcal{E}}_5\Big)\\&+\Big(\boldsymbol{PG}\boldsymbol{\mathcal{E}}_1+\boldsymbol{HPK}\widetilde{\boldsymbol{D}}\boldsymbol{\mathcal{E}}_2-\boldsymbol{HPK}\widetilde{\boldsymbol{D}}\boldsymbol{\mathcal{E}}_5\Big)^{\mathrm{T}}\boldsymbol{\mathcal{E}}_1\\&+\boldsymbol{\mathcal{E}}_1^{\mathrm{T}}\boldsymbol{Q}_1\boldsymbol{\mathcal{E}}_1-\boldsymbol{\mathcal{E}}_3^{\mathrm{T}}(\boldsymbol{Q}_1-\boldsymbol{Q}_2)\boldsymbol{\mathcal{E}}_3-\boldsymbol{\mathcal{E}}_4^{\mathrm{T}}\boldsymbol{Q}_2\boldsymbol{\mathcal{E}}_4\\&+\boldsymbol{\mathcal{E}}_{13}^{\mathrm{T}}\boldsymbol{R}_1\boldsymbol{\mathcal{E}}_{13}-\boldsymbol{\mathcal{E}}_5^{\mathrm{T}}\boldsymbol{\Phi}\boldsymbol{\mathcal{E}}_5+\boldsymbol{\Lambda}\boldsymbol{\mathcal{E}}_{25}^{\mathrm{T}}\widetilde{\boldsymbol{D}}^{\mathrm{T}}\boldsymbol{\Omega}\widetilde{\boldsymbol{D}}\boldsymbol{\mathcal{E}}_{25}\\&-\begin{bmatrix}\boldsymbol{\mathcal{E}}_{24}\\ \boldsymbol{\mathcal{E}}_{32}\end{bmatrix}^{\mathrm{T}}\begin{bmatrix}\boldsymbol{R}_2 & \boldsymbol{S}\\ \boldsymbol{S}^{\mathrm{T}} & \boldsymbol{R}_2\end{bmatrix}\begin{bmatrix}\boldsymbol{\mathcal{E}}_{24}\\ \boldsymbol{\mathcal{E}}_{32}\end{bmatrix},\\ \boldsymbol{\Gamma}=&[\boldsymbol{G},\ \ \boldsymbol{HK}\widetilde{\boldsymbol{D}},\ \ \boldsymbol{0},\ \ \boldsymbol{0},\ \ -\boldsymbol{HK}\widetilde{\boldsymbol{D}}].\end{aligned}$$

By using the Schur complement, if the following inequality

$$\begin{bmatrix}\boldsymbol{\Theta} & \tau_{\mathrm{m}}\boldsymbol{\Gamma}^{\mathrm{T}} & \delta\boldsymbol{\Gamma}^{\mathrm{T}}\\ * & -\boldsymbol{R}_1 & \boldsymbol{0}\\ * & * & -\boldsymbol{R}_2\end{bmatrix}<0 \tag{26}$$

is satisfied, then we have

$$\boldsymbol{\Theta}+\boldsymbol{\Gamma}^{\mathrm{T}}(\tau_{\mathrm{m}}^2\boldsymbol{R}_1+\delta^2\boldsymbol{R}_2)\boldsymbol{\Gamma}<0.$$

This implies that $\dot{V}(t,\boldsymbol{\theta},\dot{\boldsymbol{\theta}})<0$ is guaranteed. Finally, to obtain protocol gain matrices and event-triggering parameters, one employs $\hat{\boldsymbol{P}}=\boldsymbol{P}^{-1}$,

$\hat{\boldsymbol{Q}}_a = \hat{\boldsymbol{P}}\boldsymbol{Q}_a\hat{\boldsymbol{P}}$, $\hat{\boldsymbol{R}}_a = \hat{\boldsymbol{P}}\boldsymbol{R}_a\hat{\boldsymbol{P}}$, $\hat{\boldsymbol{\Phi}} = \hat{\boldsymbol{P}}\boldsymbol{\Phi}\hat{\boldsymbol{P}}$, $\hat{\boldsymbol{\Omega}} = \hat{\boldsymbol{P}}\widetilde{\boldsymbol{D}}^{\mathrm{T}}\boldsymbol{\Omega}\widetilde{\boldsymbol{D}}\hat{\boldsymbol{P}}$, $\hat{\boldsymbol{S}} = \hat{\boldsymbol{P}}\boldsymbol{S}\hat{\boldsymbol{P}}$, and $\hat{\boldsymbol{K}} = \hat{\boldsymbol{P}}\boldsymbol{K}\widetilde{\boldsymbol{D}}$. Pre and post multiplying both sides of inequalities (23) and (26) by

$$\mathrm{diag}\{\hat{\boldsymbol{P}}, \hat{\boldsymbol{P}}, \hat{\boldsymbol{P}}, \hat{\boldsymbol{P}}, \hat{\boldsymbol{P}}, -\boldsymbol{R}_1, -\boldsymbol{R}_2\}$$

and considering that the inequality

$$-\hat{\boldsymbol{P}}\boldsymbol{R}_a\hat{\boldsymbol{P}} \leq -2\rho_a\hat{\boldsymbol{P}} + \rho_a^2\hat{\boldsymbol{R}}_a$$

holds for $a = 1,\ 2$, one can derive inequalities (17) and (18), which completes the proof.

4 An illustrative example

In this section, to illustrate the effectiveness of the above-mentioned results, the proposed cross-dimensional event-triggered formation control protocol is applied to a group of eight agents consisting of three autonomous unicycle-type mobile robots, four quadrotors, and one leader agent.

Indices 1, 2, and 3 stand for the three mobile robots, while 4, 5, 6, and 7 represent the four quadrotors. The index of the leader is denoted as 0. For convenience, we denote $\boldsymbol{x}_i(t) = \mathrm{col}\{x_{i1}(t), x_{i2}(t)\}$ and $\boldsymbol{v}_i(t) = \mathrm{col}\{v_{i1}(t), v_{i2}(t)\}$ if $i \in \{1, 2, 3\}$, while $\boldsymbol{x}_i(t) = \mathrm{col}\{x_{i1}(t), x_{i2}(t), x_{i3}(t)\}$ and $\boldsymbol{v}_i(t) = \mathrm{col}\{v_{i1}(t), v_{i2}(t), v_{i3}(t)\}$ if $i \in \{0, 4, 5, 6, 7\}$. Thus, it is determined that $\boldsymbol{x}_i(t) \in \mathbb{R}^2$, $\boldsymbol{v}_i(t) \in \mathbb{R}^2$ if i=1, 2, 3; $\boldsymbol{x}_i(t) \in \mathbb{R}^3$, $\boldsymbol{v}_i(t) \in \mathbb{R}^3$ if i=0, 4, 5, 6, 7.

Next, we make the leader and four quadrotors (followers) fly in a cubical space with three coordinate axes (X, Y, and Z), while the three robots (followers) move in the $X-Y$ plane with $Z=-50$. The employed communication digraph is expressed in Fig. 3. For the sake of simplicity, we consider the case where there is no information interaction between follower agents with different dimensions. Thus, we

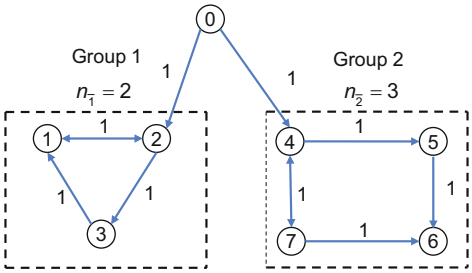

Fig. 3 Communication topology

have diagonal matrix $\widetilde{\boldsymbol{L}} = [\boldsymbol{L}_1 \otimes \boldsymbol{I}_{2n_{\bar{1}}}, \boldsymbol{L}_2 \otimes \boldsymbol{I}_{2n_{\bar{2}}}]$ with

$$\boldsymbol{L}_1 = \begin{bmatrix} 2 & -1 & -1 \\ -1 & 1 & 0 \\ 0 & -1 & 1 \end{bmatrix},\ \boldsymbol{L}_2 = \begin{bmatrix} 1 & 0 & 0 & -1 \\ -1 & 1 & 0 & 0 \\ 0 & -1 & 2 & -1 \\ -1 & 0 & 0 & 1 \end{bmatrix}.$$

Then, when the damping terms (Ma et al., 2022) are involved (damping matrices are nonzero), the system matrices of the three unicycle robots and four quadrotors can be given as

$$\boldsymbol{A}_1 = -\begin{bmatrix} 0.3 & 0 \\ 0.01 & 0.07 \end{bmatrix},\ \boldsymbol{A}_2 = -\begin{bmatrix} 0.2 & 0 \\ 0.03 & 0.06 \end{bmatrix},$$

$$\boldsymbol{A}_3 = -\begin{bmatrix} 0.4 & -0.1 \\ 0.02 & 0.04 \end{bmatrix},\ \boldsymbol{A}_4 = -\begin{bmatrix} 0.3 & 0 & 0 \\ 0.01 & 0.07 & 0 \\ 0.05 & 0 & 0.4 \end{bmatrix},$$

$$\boldsymbol{B}_1 = -\begin{bmatrix} 0.5 & 0.1 \\ 0.4 & 2 \end{bmatrix},\quad \boldsymbol{B}_2 = -\begin{bmatrix} 0.4 & 0.2 \\ 0.5 & 3 \end{bmatrix},$$

$$\boldsymbol{B}_3 = -\begin{bmatrix} 0.6 & 0.15 \\ 0.3 & 2.5 \end{bmatrix},\quad \boldsymbol{B}_4 = -\begin{bmatrix} 0.5 & 0.1 & 0 \\ 0.4 & 2 & 0 \\ 0 & 0 & 0.6 \end{bmatrix},$$

$$\boldsymbol{A}_5 = -\begin{bmatrix} 0.4 & -0.1 & 0 \\ 0.02 & 0.06 & 0 \\ 0.03 & 0 & 0.2 \end{bmatrix},$$

$$\boldsymbol{A}_6 = -\begin{bmatrix} 0.2 & -0.2 & 0 \\ 0.02 & 0.04 & -0.01 \\ 0.04 & 0 & 0.2 \end{bmatrix},$$

$$\boldsymbol{A}_7 = -\begin{bmatrix} 0.3 & 0 & 0 \\ 0.01 & 0.07 & 0 \\ 0.05 & 0 & 0.4 \end{bmatrix},$$

$$\boldsymbol{B}_5 = -\begin{bmatrix} 0.7 & 0.2 & -0.1 \\ 0.3 & 1 & 0 \\ 0 & -1 & 0.5 \end{bmatrix},$$

$$\boldsymbol{B}_6 = -\begin{bmatrix} 0.6 & 0.2 & 0 \\ 0.5 & 2.5 & -0.1 \\ 0 & -0.3 & 0.6 \end{bmatrix},$$

$$\boldsymbol{B}_7 = -\begin{bmatrix} 0.4 & 0.2 & -0.02 \\ 0.3 & 3 & 0 \\ -0.1 & 0 & 0.4 \end{bmatrix}.$$

The time-varying formation patterns of the MAS are set as $\boldsymbol{f}_i(t) = \mathrm{col}\{-50\cos(0.2t + \frac{2(i-1)\pi}{3}), -50\sin(0.2t + \frac{2(i-1)\pi}{3}), 10\sin(0.2t + \frac{2(i-1)\pi}{3}), -10\cos(0.2t + \frac{2(i-1)\pi}{3})\}$ for $i = 1, 2, 3$; $\boldsymbol{f}_4(t) = \mathrm{col}\{0, 0, 30, 0, 0, 0\}$; $\boldsymbol{f}_j(t) = \mathrm{col}\{-50\cos(0.4t + \frac{b\pi}{3}), -50\sin(0.4t + \frac{b\pi}{3}), 10,$

$20\sin(0.4t+\frac{b\pi}{3}), -20\cos(0.4t+\frac{b\pi}{3}), 0\}$ for $j=5,6,7$ and $b=1,3,5$. The initial states of the eight agents are listed in Table 1.

Table 1 Initial conditions of agents (including positions and velocities)

Agent index i	$\boldsymbol{x}_i(0)$ (m)	$\boldsymbol{v}_i(0)$ (m/s)
0	(60, 150, 20)	(1, 2, 1)
1	(100, −40)	(0.1, −3)
2	(−80, 50)	(−0.2, −0.1)
3	(0, 60)	(0.2, 0.21)
4	(30, 90, 50)	(0.1, 0.3, 0.4)
5	(50, 30, 40)	(0.3, 0.2, 0.1)
6	(80, 30, 70)	(0.3, −0.7, 0.3)
7	(20, 25, 50)	(0.3, 0.4, 0.5)

The other parameters are chosen as $\tau_{\mathrm{m}}=0.01$ s, $\tau_{\mathrm{M}}=0.04$ s, $\rho_1=0.01$, $\rho_2=0.02$, $\sigma_1=0.03$, $\sigma_2=0.02$, $\sigma_3=0.15$, $\sigma_4=0.07$, $\sigma_5=0.09$, $\sigma_6=0.09$, and $\sigma_7=0.08$. Using Theorem 1, the following formation control protocol gain matrices are derived:

$$\boldsymbol{K}_1=\begin{bmatrix}-0.0258 & -0.0091 & -0.0632 & -0.0103\\ -0.0321 & -0.1671 & -0.0049 & -0.1777\end{bmatrix},$$

$$\boldsymbol{K}_2=\begin{bmatrix}-0.0224 & -0.0085 & -0.0666 & -0.0065\\ -0.0227 & -0.1672 & 0.0023 & -0.1333\end{bmatrix},$$

$$\boldsymbol{K}_3=\begin{bmatrix}-0.0434 & -0.046 & -0.0954 & -0.0296\\ -0.0345 & -0.4661 & -0.0107 & -0.4106\end{bmatrix},$$

$$\boldsymbol{K}_4=\begin{bmatrix}\boldsymbol{K}_{41}, & \boldsymbol{K}_{42}\end{bmatrix},\ \boldsymbol{K}_5=\begin{bmatrix}\boldsymbol{K}_{51}, & \boldsymbol{K}_{52}\end{bmatrix},$$

$$\boldsymbol{K}_6=\begin{bmatrix}\boldsymbol{K}_{61}, & \boldsymbol{K}_{62}\end{bmatrix},\ \boldsymbol{K}_7=\begin{bmatrix}\boldsymbol{K}_{71}, & \boldsymbol{K}_{72}\end{bmatrix},$$

where

$$\boldsymbol{K}_{41}=\begin{bmatrix}-0.0266 & -0.0093 & 0.0004\\ -0.0330 & -0.1707 & -0.0007\\ 0.0023 & 0.0007 & -0.0206\end{bmatrix},$$

$$\boldsymbol{K}_{42}=\begin{bmatrix}-0.0650 & -0.0105 & 0.0017\\ -0.0051 & -0.1815 & 0\\ 0.0038 & 0.0009 & -0.0479\end{bmatrix},$$

$$\boldsymbol{K}_{51}=\begin{bmatrix}-0.0163 & -0.0122 & 0.0026\\ -0.0148 & -0.0812 & -0.0066\\ 0.0021 & 0.0295 & -0.0211\end{bmatrix},$$

$$\boldsymbol{K}_{52}=\begin{bmatrix}-0.0342 & -0.0077 & 0.0063\\ 0.0062 & -0.1481 & -0.0139\\ 0.0064 & 0.0033 & -0.0572\end{bmatrix},$$

$$\boldsymbol{K}_{61}=\begin{bmatrix}-0.0874 & -0.1336 & 0.0086\\ -0.0901 & -0.5584 & 0.0137\\ 0.0092 & 0.0373 & -0.0768\end{bmatrix},$$

$$\boldsymbol{K}_{62}=\begin{bmatrix}-0.1792 & -0.0804 & 0.0141\\ -0.0682 & -0.4557 & -0.0012\\ 0.0235 & 0.0137 & -0.1798\end{bmatrix},$$

$$\boldsymbol{K}_{71}=\begin{bmatrix}-0.0476 & -0.0266 & 0.0014\\ -0.0497 & -0.5008 & -0.0013\\ 0.0079 & 0.0005 & -0.0331\end{bmatrix},$$

$$\boldsymbol{K}_{72}=\begin{bmatrix}-0.1340 & -0.0179 & 0.0013\\ -0.0073 & -0.4036 & -0.0001\\ 0.0053 & 0.0005 & -0.0976\end{bmatrix}.$$

The simulation results of implementing the proposed cross-dimensional formation control protocol and event-triggered communication protocol are shown in Figs. 4–6. Specifically, the trajectories of the three unicycle robots and four quadrotors are shown in Fig. 4. The first two-dimensional velocity responses of the seven follower agents, including the unicycle mobile robots and quadrotors, are shown in Fig. 5. Fig. 6 illustrates the triggering time instants for each follower agent. There are totally 500 data packets within t=25 s, and only 32, 26, 30, 29, 36, 38, and 37 data packets respectively on followers 1–7 are transmitted through the communication network, which saves limited network resources. From Figs. 4–6, we can see that the desired formation pattern is achieved under the proposed formation control protocol and event-triggered communication protocol.

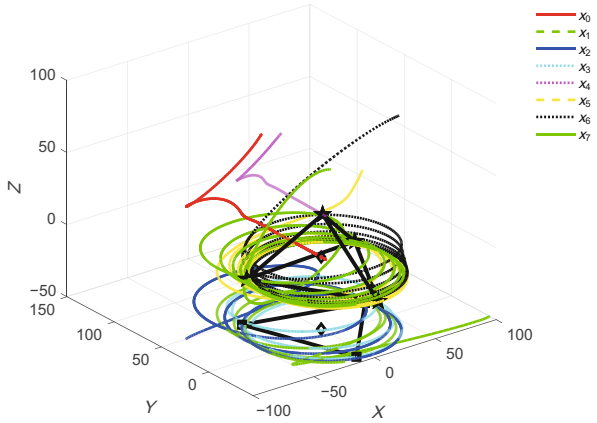

Fig. 4 Trajectories of followers and the leader

5 Conclusions

The problem of event-triggered distributed HMAS cross-dimensional formation control is tackled in our work.

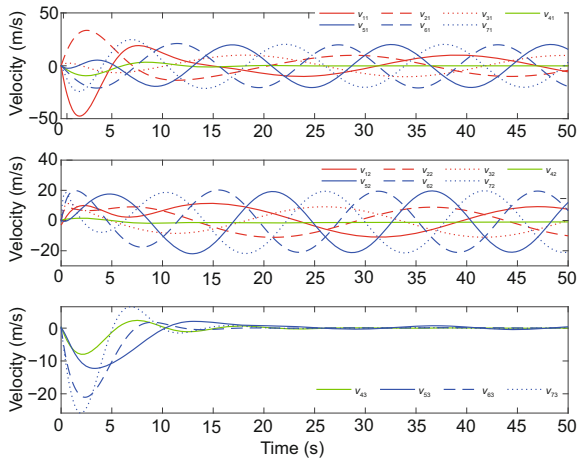

Fig. 5 X-velocity, Y-velocity of followers 1–7 and Z-velocity of followers 4–7

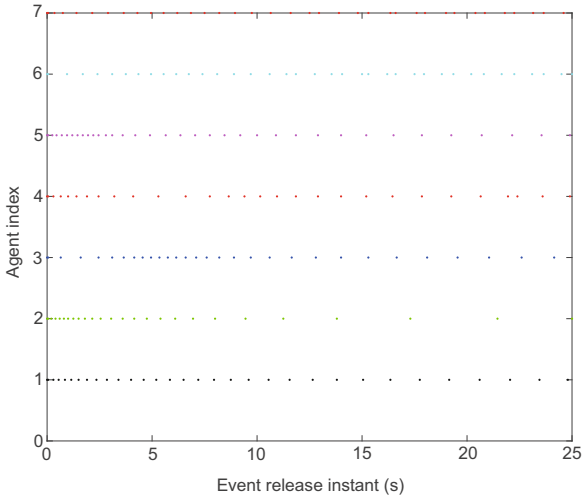

Fig. 6 Event release instants of followers 1–7

To save limited communication resources, a cross-dimensional event-triggered data transmission protocol has been proposed to schedule communication among agents with different dimensions. Leveraging the proposed cross-dimensional event-triggered communication protocol, the cross-dimensional formation of an HMAS has achieved the asymptotic stability of a closed-loop error system. Then, to facilitate the design of a cross-dimensional formation control protocol and event-triggered weighting parameters when there is no information interaction between follower agents with different dimensions, several criteria have been proposed. Finally, a simulation study case has been implemented to substantiate the efficacy of the designed protocol.

Contributors

Huimin WEI designed the research and drafted the paper. Chen PENG helped organize the paper. Huimin WEI, Chen PENG, and Min ZHAO revised and finalized the paper.

Conflict of interest

All the authors declare that they have no conflict of interest.

Data availability

The data that support the findings of this study are available from the corresponding author upon reasonable request.

References

Ding L, Zheng WX, 2017. Network-based practical consensus of heterogeneous nonlinear multiagent systems. *IEEE Trans Cybern*, 47(8):1841-1851. https://doi.org/10.1109/TCYB.2016.2601488

Dong XW, Yu BC, Shi ZY, et al., 2015. Time-varying formation control for unmanned aerial vehicles: theories and applications. *IEEE Trans Contr Syst Technol*, 23(1): 340-348. https://doi.org/10.1109/TCST.2014.2314460

Dou LY, Song C, Wang XF, et al., 2020. Target localization and enclosing control for networked mobile agents with bearing measurements. *Automatica*, 118:109022. https://doi.org/10.1016/j.automatica.2020.109022

Ge XH, Han QL, 2015. Distributed event-triggered H_∞ filtering over sensor networks with communication delays. *Inform Sci*, 291:128-142. https://doi.org/10.1016/j.ins.2014.08.047

Ge XH, Han QL, 2017. Distributed formation control of networked multi-agent systems using a dynamic event-triggered communication mechanism. *IEEE Trans Ind Electron*, 64(10):8118-8127. https://doi.org/10.1109/TIE.2017.2701778

Ge XH, Xiao SY, Han QL, et al., 2022. Dynamic event-triggered scheduling and platooning control co-design for automated vehicles over vehicular ad-hoc networks. *IEEE/CAA J Autom Sin*, 9(1):31-46. https://doi.org/10.1109/JAS.2021.1004060

Ge XH, Han QL, Wu Q, et al., 2023. Resilient and safe platooning control of connected automated vehicles against intermittent denial-of-service attacks. *IEEE/CAA J Autom Sin*, 10(5):1234-1251. https://doi.org/10.1109/JAS.2022.105845

Ge XH, Han QL, Zhang XM, et al., 2024. Communication resource-efficient vehicle platooning control with various spacing policies. *IEEE/CAA J Autom Sin*, 11(2):362-376. https://doi.org/10.1109/JAS.2023.123507

Haghshenas H, Badamchizadeh MA, Baradarannia M, 2015. Containment control of heterogeneous linear multi-agent systems. *Automatica*, 54:210-216. https://doi.org/10.1016/j.automatica.2015.02.002

Hu WF, Liu L, Feng G, 2017. Output consensus of heterogeneous linear multi-agent systems by distributed event-triggered/self-triggered strategy. *IEEE Trans Cybern*,

47(8):1914-1924.
https://doi.org/10.1109/TCYB.2016.2602327

Jiang W, Wen GG, Peng ZX, et al., 2019. Fully distributed formation-containment control of heterogeneous linear multiagent systems. *IEEE Trans Automat Contr*, 64(9): 3889-3896. https://doi.org/10.1109/TAC.2018.2887409

Jiao Q, Modares H, Lewis FL, et al., 2016. Distributed L_2-gain output-feedback control of homogeneous and heterogeneous systems. *Automatica*, 71:361-368. https://doi.org/10.1016/j.automatica.2016.04.025

Ju YM, Ding DR, He X, et al., 2022. Consensus control of multi-agent systems using fault-estimation-in-the-loop: dynamic event-triggered case. *IEEE/CAA J Autom Sin*, 9(8):1440-1451. https://doi.org/10.1109/JAS.2021.1004386

Li SB, Feng G, Luo XY, et al., 2015. Output consensus of heterogeneous linear discrete-time multiagent systems with structural uncertainties. *IEEE Trans Cybern*, 45(12):2868-2879. https://doi.org/10.1109/TCYB.2015.2388538

Ma L, Wang YL, Fei MR, et al., 2022. Cross-dimensional formation control of second-order heterogeneous multi-agent systems. *ISA Trans*, 127:188-196. https://doi.org/10.1016/j.isatra.2022.02.036

Meng ZY, Yang T, Dimarogonas DV, et al., 2015. Coordinated output regulation of heterogeneous linear systems under switching topologies. *Automatica*, 53:362-368. https://doi.org/10.1016/j.automatica.2015.01.009

Ning BD, Han QL, Zuo ZY, et al., 2023. Fixed-time and prescribed-time consensus control of multiagent systems and its applications: a survey of recent trends and methodologies. *IEEE Trans Ind Inform*, 19(2):1121-1135. https://doi.org/10.1109/TII.2022.3201589

Oh KK, Park MC, Ahn HS, 2015. A survey of multi-agent formation control. *Automatica*, 53:424-440. https://doi.org/10.1016/j.automatica.2014.10.022

Park P, Ko JW, Jeong C, 2011. Reciprocally convex approach to stability of systems with time-varying delays. *Automatica*, 47(1):235-238. https://doi.org/10.1016/j.automatica.2010.10.014

Rezaee H, Abdollahi F, 2015. Pursuit formation of double-integrator dynamics using consensus control approach. *IEEE Trans Ind Electron*, 62(7):4249-4256. https://doi.org/10.1109/TIE.2014.2384479

Song WZ, Feng J, Zhang HG, et al., 2022. Event-based formation control of heterogeneous multiagent systems with leader agent of nonzero input. *Inform Sci*, 598:157-181. https://doi.org/10.1016/j.ins.2022.03.057

Song WZ, Feng J, Zhang HG, et al., 2023. Dynamic event-triggered formation control for heterogeneous multi-agent systems with nonautonomous leader agent. *IEEE Trans Neur Netw Learn Syst*, 34(12):9685-9699. https://doi.org/10.1109/TNNLS.2022.3159669

Weimerskirch H, Martin J, Clerquin Y, et al., 2001. Energy saving in flight formation. *Nature*, 413(6857):697-698. https://doi.org/10.1038/35099670

Xia LN, Li Q, Song RZ, et al., 2023. Dynamic event-triggered leader-follower control for multiagent systems subject to input time delay. *IEEE Trans Syst Man Cybern Syst*, 53(3):1970-1981. https://doi.org/10.1109/TSMC.2022.3210709

Xie ML, Ding DR, Ge XH, et al., 2024. Distributed platooning control of automated vehicles subject to replay attacks based on proportional integral observers. *IEEE/CAA J Autom Sin*, 11(9):1954-1966. https://doi.org/10.1109/JAS.2022.105941

Yang Y, Xiao Y, Li TS, 2022. Attacks on formation control for multiagent systems. *IEEE Trans Cybern*, 52(12): 12805-12817. https://doi.org/10.1109/TCYB.2021.3089375

Yang YP, Li SR, Ge XH, et al., 2024. Event-triggered cluster consensus of multi-agent systems via a modified genetic algorithm. *IEEE Trans Neur Netw Learn Syst*, 35(5): 6792-6805. https://doi.org/10.1109/TNNLS.2022.3212967

Zhang D, Xu ZH, Karimi HR, et al., 2018. Distributed H_∞ output-feedback control for consensus of heterogeneous linear multiagent systems with aperiodic sampled-data communications. *IEEE Trans Ind Electron*, 65(5):4145-4155. https://doi.org/10.1109/TIE.2017.2772196

Zhang XM, Han QL, Ge XH, et al., 2023. Sampled-data control systems with non-uniform sampling: a survey of methods and trends. *Annu Rev Contr*, 55:70-91. https://doi.org/10.1016/j.arcontrol.2023.03.004

Zhao M, Peng C, He WL, et al., 2018. Event-triggered communication for leader-following consensus of second-order multiagent systems. *IEEE Trans Cybern*, 48(6): 1888-1897. https://doi.org/10.1109/TCYB.2017.2716970